Supplementary information

A

KEGG pathway	p-value FDR	n*
focal adhesion	1.0e-6	27
pathway in cancer	1.4e-6	34
B► PI3K-Akt signaling pathway	4.3e-6	34
C► insulin signaling pathway	4.3e-6	20
microRNAs in cancer	5.0e-5	20

GO cellular component	p-value FDR	n*
intracellular	2.4e-31	545
intracellular part	4.8e-31	535
intracellular organelle	3.4e-29	489
membrane-bound organelle	1.2e-28	496
organelle	1.7e-28	517

B

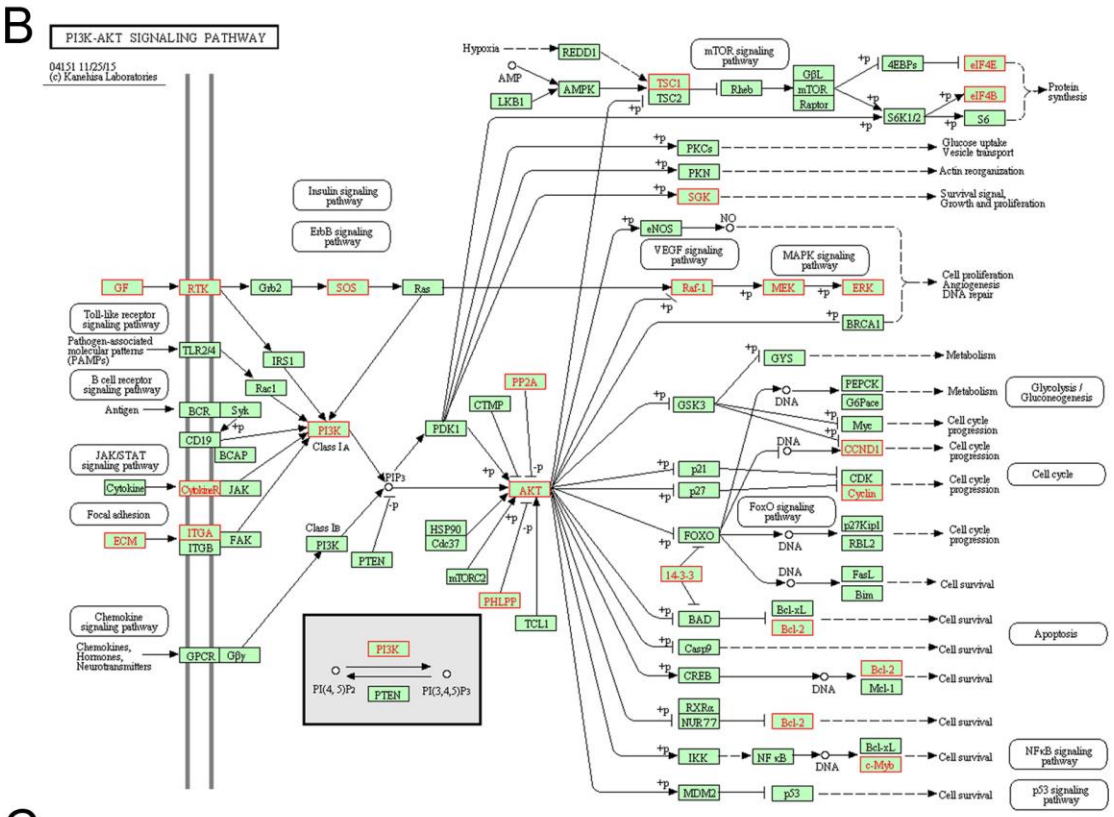

C

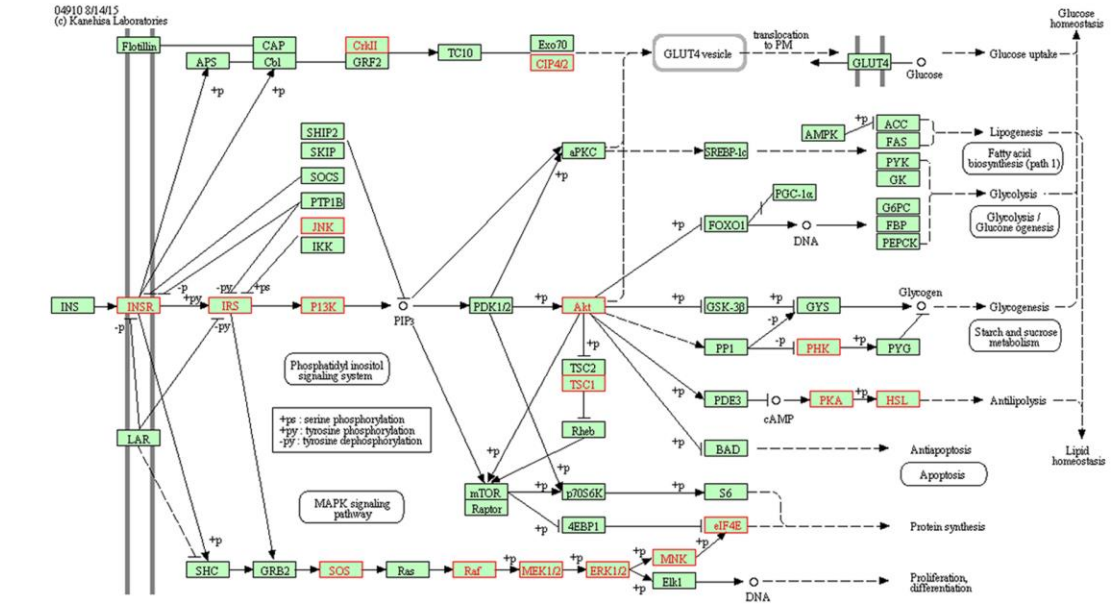

Supplemental figure 1
KEGG and GO cellular component analysis of miR-322 target genes expressed in growth plate cartilage

(A) String database analysis of expressed target genes (Szklarczyk et al., 2015). The highest ranked KEGG pathway and GO cellular component terms are shown. Significance and entity numbers are given. (B) Illustration of the PI3K-AKT and (C) insulin signaling pathway according to KEGG(Kanehisa et al., 2015). Predicted targets are labeled (red).

A

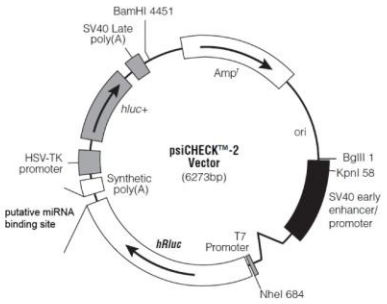

B

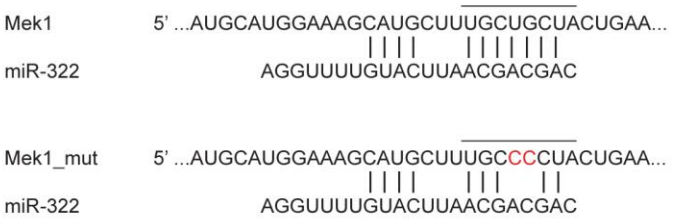

C

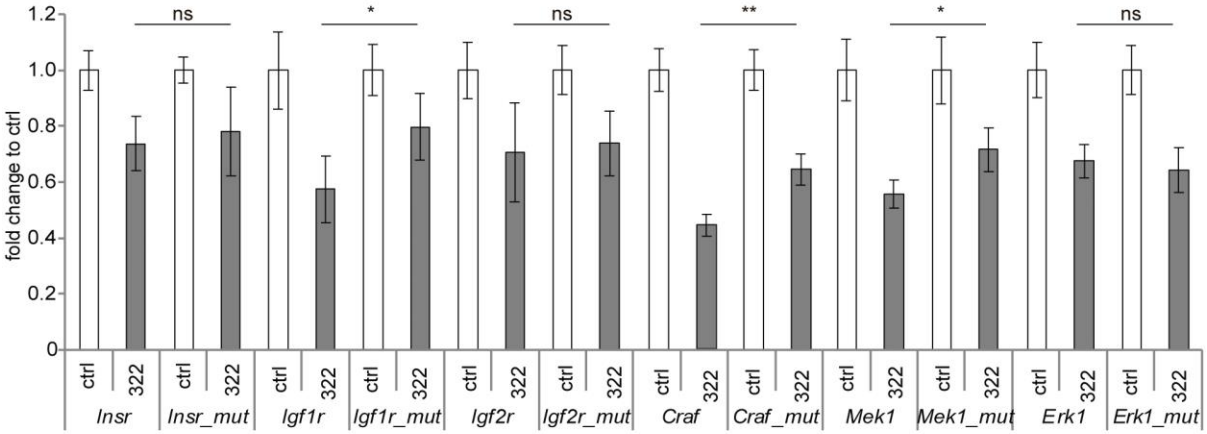

D

Primer	Sequence (5'-3')
Insr fw	cgcCCTCAAATTGACCAATAGCTGCTGCTTTCATAgc
Insr rev	ggccgcTATGAAAGCAGCAGCTATTGGTCAATTTGAGGgcgat
Insr_mut fw	cgcCCTCAAATTGACCAATAGCTGCAACTTTCATAgc
Insr_mut rev	ggccgcTATGAAAGTTGCAGCTATTGGTCAATTTGAGGgcgat
Igf1r fw	cgcATCTGTACAGGAAAAGAAAAGCTGCTATTTTTgc
Igf1r rev	ggccgcAAAAATAGCAGCTTTTCTTTTCCTGTACAGATgcgat
Igf1r_mut fw	cgcATCTGTACAGGAAAAGAAAAGCCACTATTTTTgc
Igf1r_mut rev	ggccgcAAAAATAGTGGCTTTTCTTTTCCTGTACAGATgcgat
Igf2r fw	cgcTGTGTTTGAAAAAAACCCTTGCTGCTTTAGACgc
Igf2r rev	ggccgcGTCTAAAGCAGCAAGGGTTTTTTTCAAACACAgcgat
Igf2r_mut fw	cgcTGTGTTTGAAAAAAACCCTTACTACTTTAGACgc
Igf2r_mut rev	ggccgcGTCTAAAGTAGTAAGGGTTTTTTTCAAACACAgcgat
Craf fw	tcgagATGTTTTTGGAAAAGCTGCTGCTGCTAAGGACgc
Craf rev	ggccgcGTCCTTAGCAGCAGCAGCTTTTCCAAAAACATc
Craf_mut fw	tcgagATGTTTTTGGAAAAGCTGCTGCCCTAAGGACgc
Craf_mut rev	ggccgcGTCCTTAGGGGCAGCAGCTTTTCCAAAAACATc
Mek1 fw	tcgagATGCATGGAAAGCATGCTTTGCTGCTACTGAAgc
Mek1 rev	ggccgcTTCAGTAGCAGCAAAGCATGCTTTCCATGCATc
Mek1_mut fw	tcgagATGCATGGAAAGCATGCTTTGCCCCTACTGAAgc
Mek1_mut rev	ggccgcTTCAGTAGGGGCAAAGCATGCTTTCCATGCATc
Erk1 fw	tcgagCTGCCACATGTAACGCCCTTGCTGCTTCTGTGgc
Erk1 rev	ggccgcCACAGAAGCAGCAAGGGCGTTACATGTGGCAGc
Erk1_mut fw	tcgagCTGCCACATGTAACGCCCTTGCCCCTTCTGTGgc
Erk1_mut rev	ggccgcCACAGAAGGGGCAAGGGCGTTACATGTGGCAGc

Supplemental figure 2
Luciferase miRNA:mRNA interaction assays
(A) Vector map of the psiCHECK2 Vector including the coding sequence of Renilla luciferase (hRluc), the multiple cloning site and the Firefly luciferase (hluc). (B) Illustration of the miR-322 and miR-322_mut interaction with the predicted binding sequence in the 3'-UTR of Mek1. (C) Fold changes of Renilla to Firefly luciferase activity in miR-322 mimic-transfected HEK293 cells compared to control are presented (n≥3) and control values with standard deviations are given (not shown in the Figure 2B due to space limitations). (D) Oligonucleotides used for the generation of luciferase reporter constructs containing the putative or mutated (red) miR-322 binding site are listed.

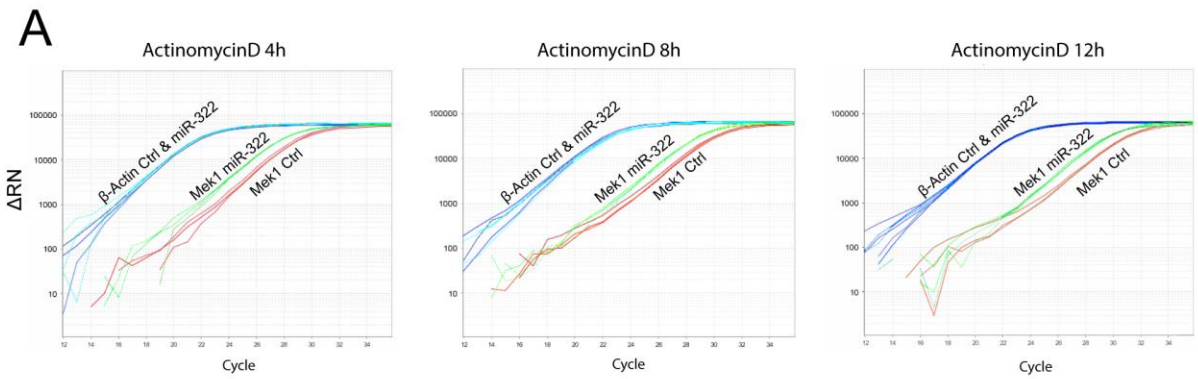

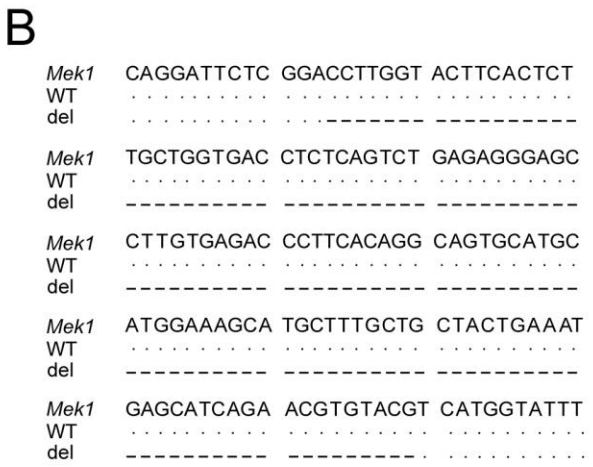

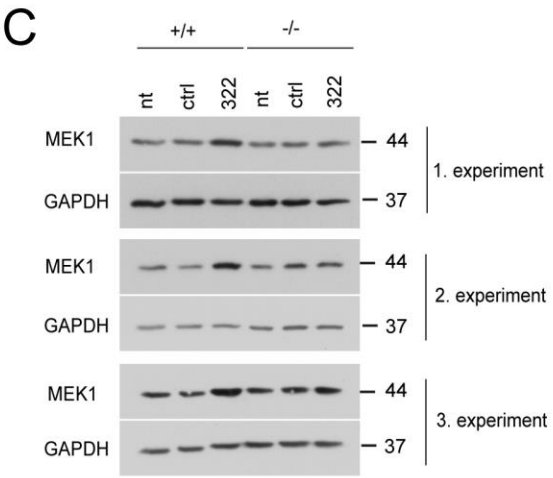

D

Primer	Sequence (5'-3')
Mek1UTR-5'-miR-322bs fw	caccgTTGTCAGGATTCTCGGACCT
Mek1UTR-5'-miR-322bs rev	aaacAGGTCCGAGAATCCTGACAAc
Mek1UTR-3'-miR-322bs fw	caccGCATCAGAACGTGTACGTCA
Mek1UTR-3'-miR-322bs rev	aaacTGACGTACACGTTCTGATGC
genotyping for	GGAATTCTCTGCCCAGTGGCATGCC
genotyping rev	GACTGAAGCCCAGCTATCATGGC

Supplemental figure 3
qPCR analysis of mir-322 expression in actinomycin D treated mimic transfected chondrocytes

(A) Ct-plots of qPCR analysis for ß-Actin (blue), Mek1 expression in control-(red) and miR-322 mimic-transfected (green) PECs four, eight and 12 hours after blocking transcription with actinomycin D. (B) The wild type sequence in the 3'UTR of *Mek1* is shown and the targeted sequence is marked (del, -) (C) Immunoblot analysis of total MEK1 and GAPDH levels in control and miR-322 mimic transfected ATDC5 cells containing the wild type (+/+) or biallelic deletion (-/-) of the miR-322 binding site in the 3'-UTR of *Mek1*. Three independent transfection experiments are shown. (D) Oligonucleotides used for CRISPR/Cas-mediated genomic manipulation and PCR-based genotyping are listed.

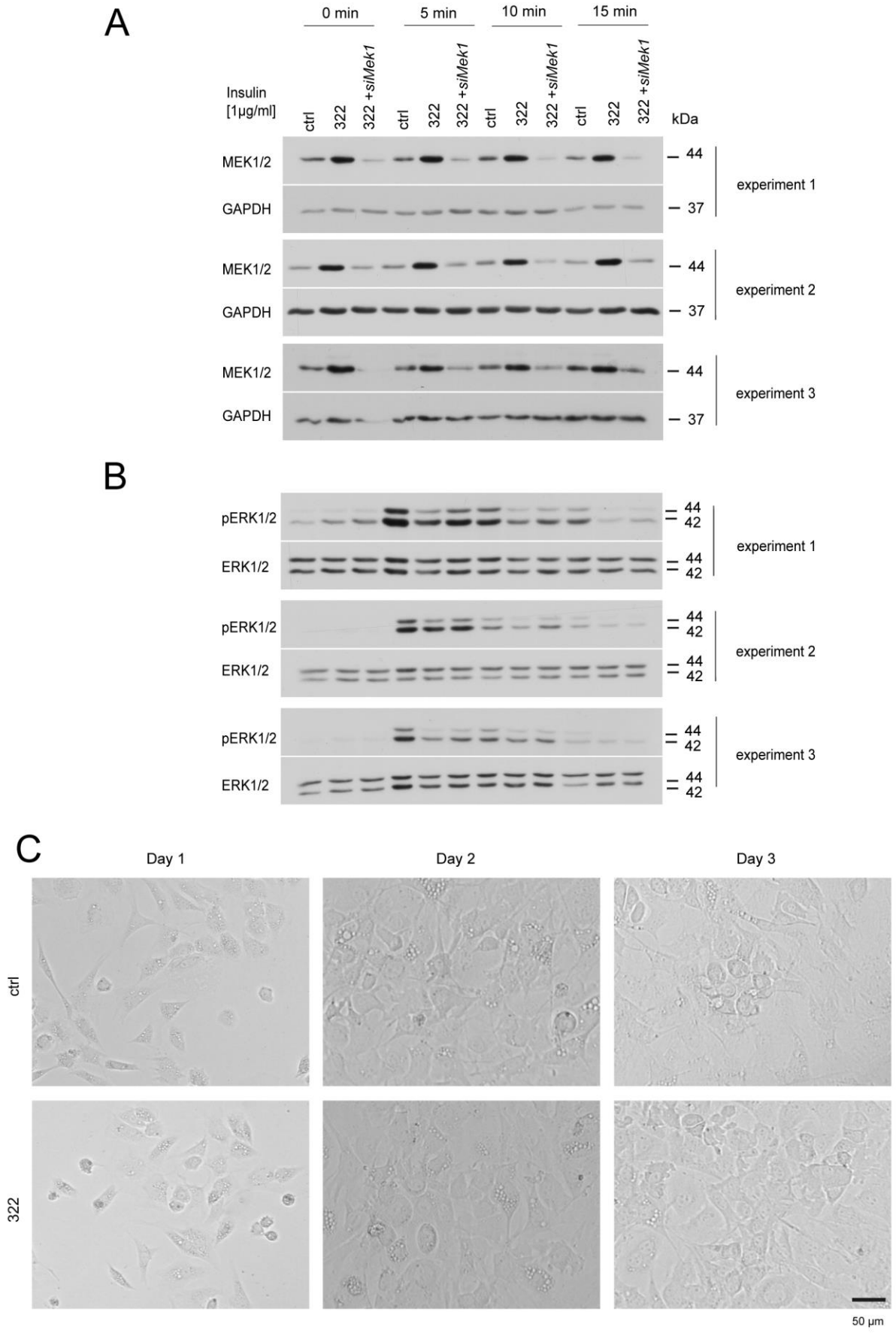

Supplemental figure 4

Reduction of MEK1 protein levels and stimulation of RAF/MEK/ERK pathway activation ERK in miR-322 mimic-transfected chondrocytes using Mek1-specific siRNA

Immunoblots showing (A) total MEK1/2 and GAPDH or (B) pERK1/2 and total ERK1/2 (lower panel) in control-, miR-322 mimic- and miR-322 mimic/MEK1-siRNA-transfected PECs of three independent experiments. (C) Representative images of control- and miR-322 mimic-transfected PEC are shown for one, two and three days after transfection. No significant differences between control- and miR-322 mimic-transfected PEC were observed. Bar: (C) 50µm

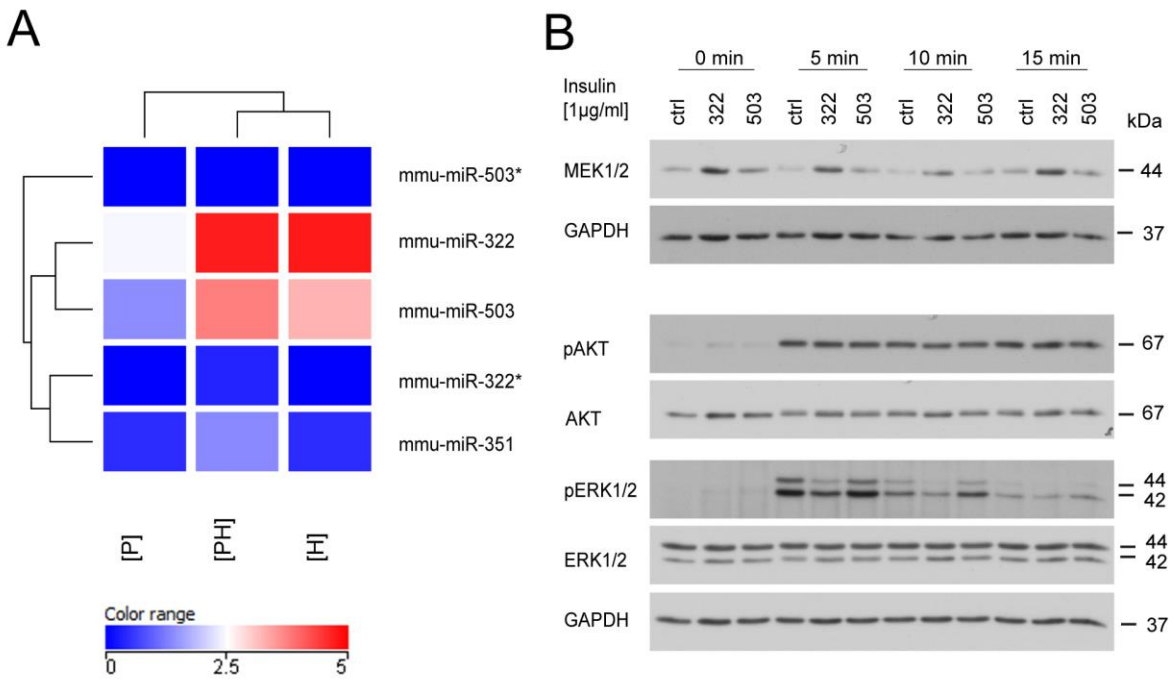

Supplemental figure 5

(A) Intensity plots of miR-322-cluster specific miRNA expression. High (red) and low (blue) expression values are indicated. (B) Representative immunoblot analysis of pMEK1/2, total MEK1/2, pERK1/2, total ERK1/2, pAKT, total AKT and GAPDH in protein levels in control-, miR-322 mimic- or miR-503 mimic- transfected primary epiphyseal chondrocytes.

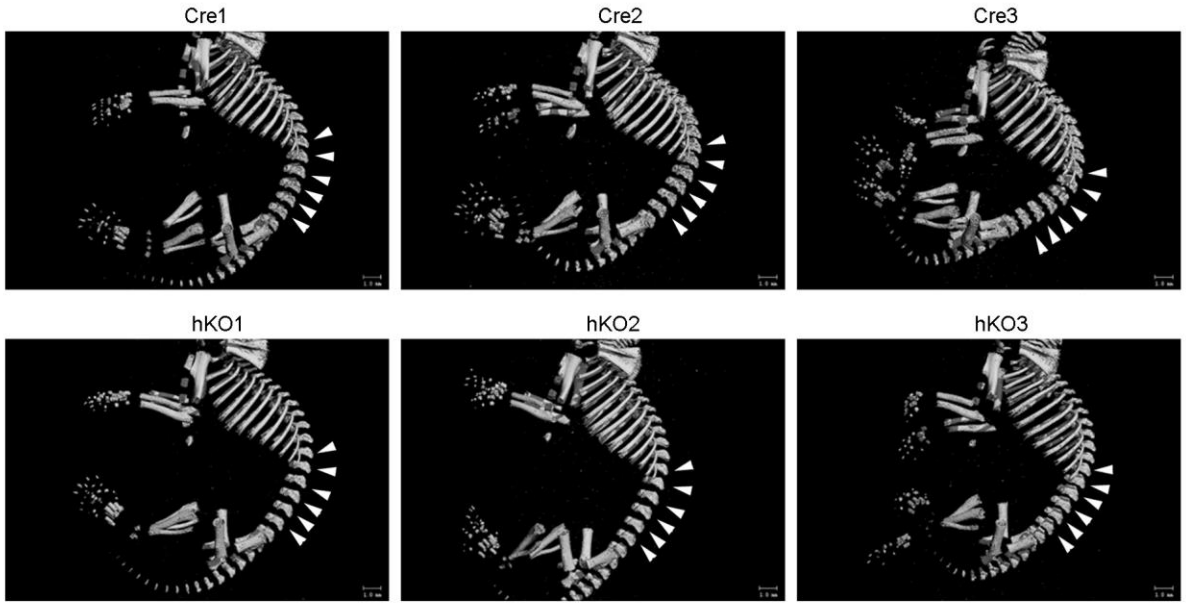

Supplemental figure 6
Visualization of the skeleton in newborns
Bony elements in newborn Col2a1-Cre (Cre) and Col2a1-Cre-*Mirc24*^{tm1M} (hKO) males (n=3 per genotype) were detected by µCT analysis. Three dimensional reconstructions are shown and the vertebral bodies are marked (arrowhead) and point to differences between the genotypes. Bars: 1mm.

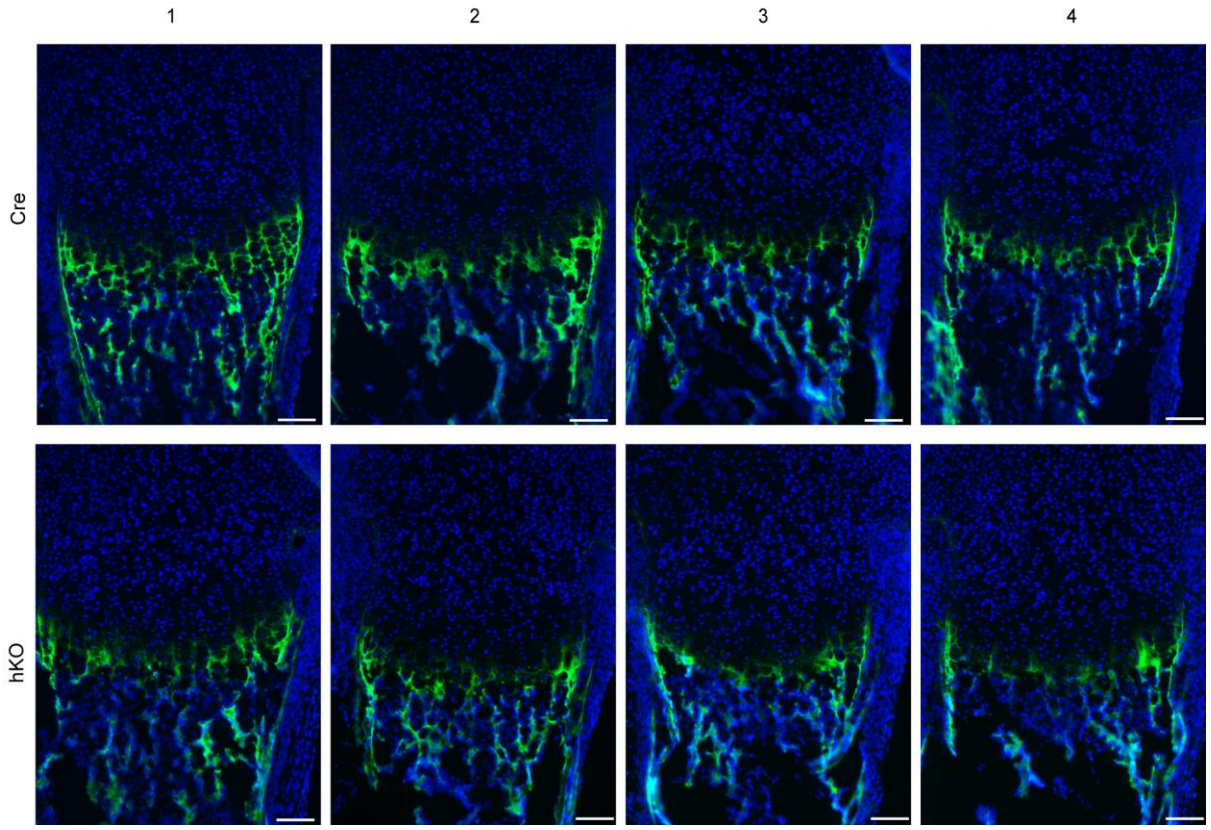

Supplemental figure 7
Characterization of the hypertrophic growth plate cartilage in newborns
Collagen X protein was detected by immunostaining (green) in the newborn growth plate cartilage of Col2a1-Cre (Cre) and Col2a1-Cre-*Mirc24*^{tm1M} (hKO) males (n=4 per genotype). Nuclei were stained with DAPI (blue). Bar: 100µm